Evolution of complex singularities in Kida–Pelz and Taylor–Green inviscid flows

C. Cichowlas, M.-E. Brachet*

Laboratoire de Physique Statistique de l'Ecole Normale Supérieure, associé au CNRS et aux Universités Paris VI et VII, 24 Rue Lhomond, 75231 Paris, France

Communicated by S. Kida

Abstract

The analyticity strip method is used to trace complex singularities in direct numerical simulations of the Kida–Pelz and Taylor–Green flows, performed with up to 2048^3 collocation points. Oscillations found in the Kida–Pelz energy spectrum are attributed to interferences of complex singularities. A generalized least-square fit that separates out the oscillations from the measure of the width of the analyticity strip δ is introduced. Using the available resolution, δ is found to decay exponentially in time up to $t = 1.25$. It is argued that resolutions in the range 16384^3–32768^3 (within reach of the Earth Simulator) are needed to really probe the Pelz singularity at $t \sim 2$.
© 2005 Published by The Japan Society of Fluid Mechanics and Elsevier B.V. All rights reserved.

1. Introduction

The existence of a finite-time infinite-vorticity singularity in three-dimensional incompressible Euler flow developing from smooth initial conditions is still an open mathematical problem (Frisch et al., 2003).

---

* Corresponding author. Tel.: +33 144323761; fax: +33 144323433.
E-mail address: marc_brachet@noos.fr (M.-E. Brachet).

One possible approach to this problem is the so-called analyticity strip method (Sulem et al., 1983). The basic idea of this method is to trace complex singularities numerically on direct numerical simulations (DNS) of the Euler equation with enough spatial resolution to capture the exponential tails in the Fourier transforms. The logarithmic decrement of the energy spectrum at high-k is twice the width $\delta(t)$ of the analyticity strip of the velocity field and the problem of blowup reduces to check if $\delta(t)$ vanishes in a finite time.

This method has been applied to three-dimensional Euler flows generated by the Taylor and Green (1937) (TG) initial conditions, with resolutions 256^3 (Brachet et al., 1983) and 864^3 (Brachet et al., 1992). It was observed that, after an early transient period, the width of the analyticity strip of the velocity field decayed exponentially in time.

The Kida–Pelz (KP) flow was introduced by Kida (1985). It has all the symmetries of the TG vortex and also displays additional symmetries that make it invariant under the full octahedral group (Pelz, 2001). This flow was used by Pelz (2003), Pelz and Gulak (1997a, b), Boratav and Pelz (1994b) to study the problem of Euler blowup, using temporal Taylor series expansions. It was also used by Boratav and Pelz (1994a) to make DNS of viscous turbulence.

It has been argued by Kerr (1993) that more symmetries than the ones present in the TG vortex are needed in order to observe a singularity. Thus, the KP flow could well be a better candidate for finite time singularity than the TG flow.

The main purpose of this paper is to apply the analyticity strip method to DNS of the TG and KP flows with resolutions up to 2048^3. It will turn out to be necessary to generalize the least square fit used to extract $\delta(t)$ from the energy spectrum so that the fit takes into account oscillations that are found in the KP energy spectrum.

The paper is organized as follows. Section 2 contains a short description of the (standard) numerical methods used to integrate the Euler equation. Section 3 contains the generalization of the least square fit and numerical results. Finally Section 4 is our conclusion.

2. Numerical approach

The three-dimensional incompressible Euler equations,

$$\frac{\partial \mathbf{v}}{\partial t} + (\mathbf{v} \cdot \nabla)\mathbf{v} = -\nabla p, \tag{1}$$

$$\nabla \cdot \mathbf{v} = 0 \tag{2}$$

with (2π-periodic) initial data are solved numerically using standard (Gottlieb and Orszag, 1977) pseudo-spectral methods with resolution N. Time marching is done with a second-order leapfrog finite-difference scheme. The solutions are dealiased by suppressing, at each time step, the modes for which at least one wave-vector component exceeds two-thirds of the maximum wave-number $N/2$ (thus a 2048^3 run is truncated at $k_{max} = 682$). Symmetries are used in a standard way (Brachet et al., 1983) to reduce memory storage and speed up computations.

Two types of computations, corresponding to different initial conditions, are carried out. The first type concerns the Taylor–Green vortex (Taylor and Green, 1937) which is the incompressible

three-dimensional flow developing from the single-mode initial data

$$u^{\text{TG}} = \sin(x)\cos(y)\cos(z), \quad v^{\text{TG}} = -u^{\text{TG}}(y, -x, z), \quad w^{\text{TG}} = 0. \tag{3}$$

The second type of runs concerns the Kida–Pelz (Kida, 1985; Pelz, 2001; Boratav and Pelz, 1994b) flow, that develops from the initial data

$$u^{\text{KP}} = \sin(x)(\cos(3y)\cos(z) - \cos(y)\cos(3z)), \quad v^{\text{KP}} = u^{\text{KP}}(y, z, x), \quad w^{\text{KP}} = u^{\text{KP}}(z, x, y). \tag{4}$$

Series of runs are made for the two flows by varying the resolution N.

Two quantities are extracted from the runs, in order to monitor the time-evolution of the flows. The energy spectrum is defined by averaging $\hat{\mathbf{v}}(\mathbf{k}', t)$ (the spatial Fourier transform of the solution to Eq. (1)) on spherical shells of width $\Delta k = 1$,

$$E(k, t) = \frac{1}{2} \sum_{k - \Delta k/2 < |\mathbf{k}'| < k + \Delta k/2} |\hat{\mathbf{v}}(\mathbf{k}', t)|^2 \tag{5}$$
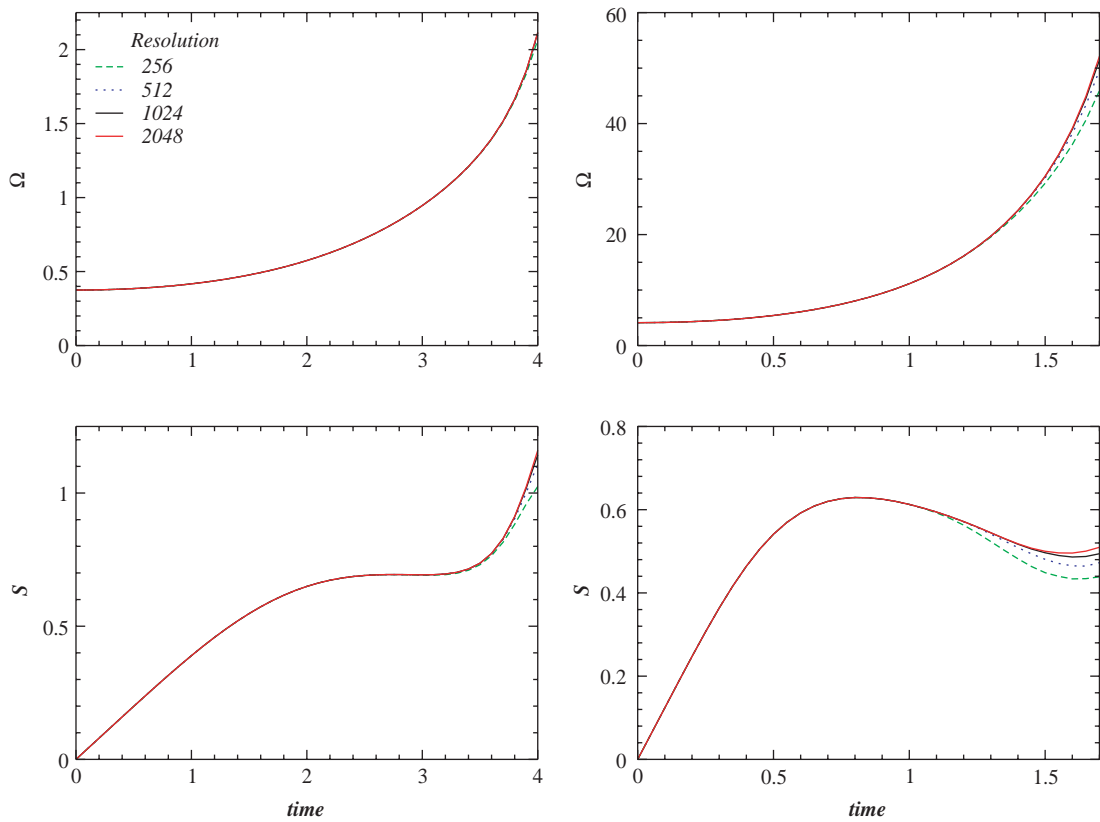

Fig. 1. Enstrophy $\Omega(t)$ and its normalized time derivative $S(t)$ (see Eq. (7)) for the TG flow (left) and KP flow (right) at various resolutions.

and the enstrophy $\Omega(t) = \int_0^\infty k^2 E(k, t)\, \mathrm{d}k$, that is computed directly (i.e. without shell averaging) as

$$\Omega(t) = \frac{1}{2} \sum_{\mathbf{k}'} |\hat{\mathbf{v}}(\mathbf{k}', t)|^2 \mathbf{k}'^2. \tag{6}$$

Fig. 1 displays the time variation of the enstrophy $\Omega(t)$ and of its normalized time derivative

$$S(t) = \left(\frac{135}{98}\right)^{1/2} \Omega^{-3/2} \frac{\mathrm{d}\Omega}{\mathrm{d}t} \tag{7}$$

(which identifies with the skewness when isotropy is assumed (Brachet et al., 1983)).

Note that (7) implies $\Omega(t)^{-1/2} = \Omega(0)^{-1/2} - (392/135)^{1/2} \int_0^t \mathrm{d}s\, S(s)$. Thus $S(t)$ should tend to zero when t goes to infinity in order to prevent a finite-time blowup of the enstrophy. Such a decay is not visible in Fig. 1. The integration time is in fact too short to reveal the asymptotic behavior of S and Ω. We will see below that more resolution is needed to extend the integration time.

3. Tracing complex singularities

When the velocity field is analytic, the energy spectrum $E(k, t)$ decays exponentially at large k (with a possible algebraic prefactor). The logarithmic decrement is twice the width $\delta(t)$ of the analyticity strip of the solution continued to complex spatial variables. The basic idea of the analyticity strip method (Sulem et al., 1983) is to trace the temporal behavior of $\delta(t)$ in order to obtain evidence for or against blowup.

In order to extract $\delta(t)$ from the numerical integrations a least-square fit is performed on the logarithm of the computed energy spectrum, using the functional form

$$\log(E(k, t)) = C - n \log(k) - 2\delta k. \tag{8}$$

The error on the fit interval $k_1 \leqslant k \leqslant k_2$,

$$\chi^2 = \sum_{k_1 \leqslant k_i \leqslant k_2} (\log(E(k_i, t)) - (C - n \log(k_i) - 2\delta k_i))^2 \tag{9}$$

is minimized by solving the equations $\partial \chi^2 / \partial C = 0$, $\partial \chi^2 / \partial n = 0$ and $\partial \chi^2 / \partial \delta = 0$. Note that these equations are linear in the fit parameters C, n and δ.

Examples of KP and TG energy spectra to be fitted in such a way are presented in Fig. 2. It is apparent on the figure that resolution-dependent spectral even–odd oscillations are present, at certain times, on the TG energy spectrum. Note that this behavior is controlled by the round-off error $\sim 10^{-15}$. For a given precision and resolution, the maximum time up to which the simulation is reliable should be the first instance at which the value of the spectrum at the highest wavenumber becomes comparable to the square of the round-off error. However, these round-off errors only affect the highest wavenumbers of the TG energy spectrum. They are eliminated by averaging the TG spectrum on shells of width $\Delta k = 2$ before performing the fit (Brachet et al., 1983). Note that longer period oscillations are visible on the KP energy spectra, but that no strong resolution-dependent effect can be seen.

The measure of $\delta(t)$ is reliable as long as it remains larger than a few mesh sizes, a condition required for the smallest scales to be accurately resolved and spectral convergence ensured. Thus only the fits giving a value of δ such that $\delta k_{\max} > 2$ will be considered.
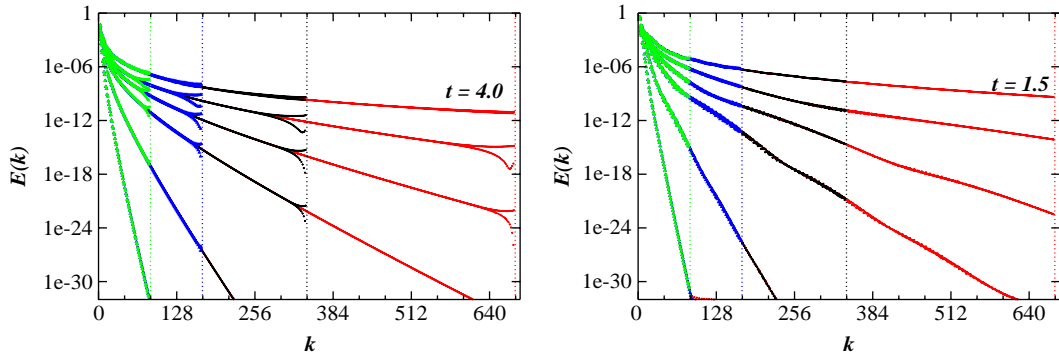
Fig. 2. Energy spectra at resolutions 256^3, 512^3, 1024^3 and 2048^3; the spectral cut-off is indicated, for each resolution, by the vertical dotted-lines. Left TG flow at $t = (1.3, 1.9, 2.5, 2.9, 3.4, 4.0)$; right KP flow at $t = (0.25, 0.5, 0.75, 0.9, 1.1, 1.5)$.
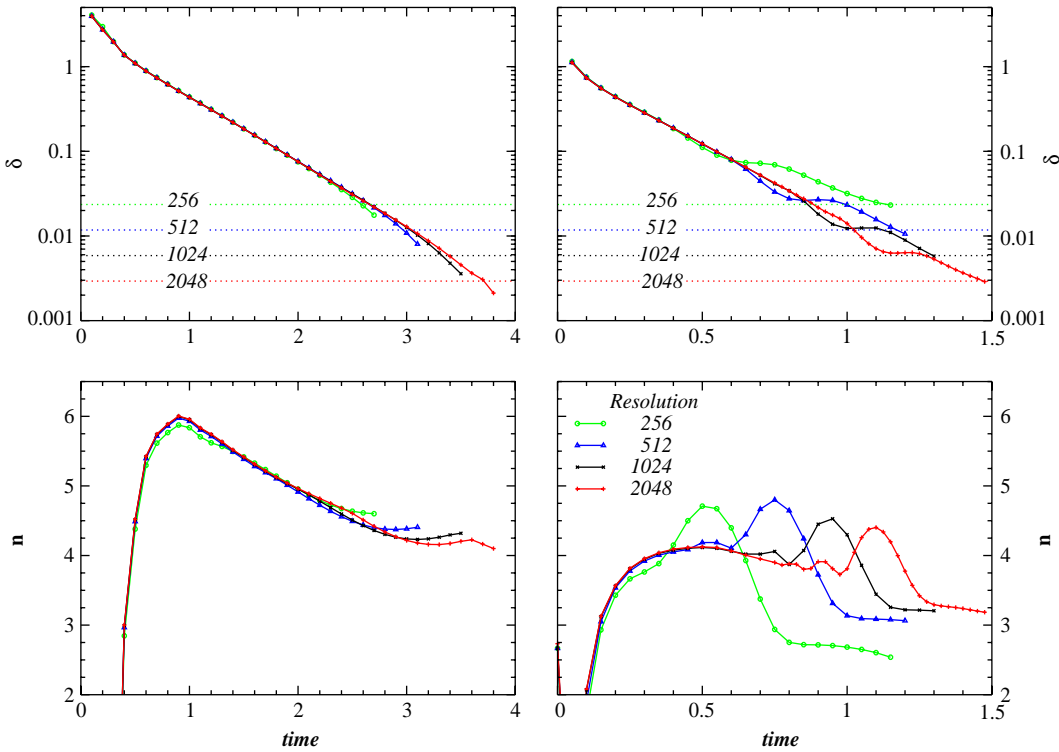

Fig. 3. Time evolution of decrement δ and prefactor n for TG flow (left) and KP flow (right) at various resolutions (see Eq. (8)). Fits are performed within the intervals $k = 5$ to $\min(k^*, N/3)$, where $k^* = \min_{E(k) < 10^{-32}}(k)$ marks the beginning of roundoff noise at short times.

Fig. 3 displays the values of δ and n for the TG and KP flows. It is visible that, after a short transient period, the TG flow $\delta(t)$ decays like

$$\delta(t) = \delta_0^{\mathrm{TG}} e^{-t/T_{\mathrm{TG}}} \tag{10}$$

with a characteristic decay time $T_{\mathrm{TG}} = 0.56$ and $\delta_0^{\mathrm{TG}} = 2.70$, up to a time $t = 3.7$ at resolution 2048^3 when it becomes comparable to twice the smallest resolved scale.

In contrast, it is apparent on the right pannels of Fig. 3 that the behavior of δ and n in the KP flow is erratic and that their values are not stable when the resolution is changed. This happens even though the higher resolution energy spectrum has identical low-wavenumber values than the lower resolution energy spectrum (see Fig. 2). This kind of behavior is possible only if some kind of systematic error is present in the fit procedure. It is plausible that this error comes from the long period oscillations slightly visible on the KP energy spectra displayed in Fig. 2.

In order to take this oscillation into account, we generalize the functional form of (8) to

$$\log(E(k,t)) = C - n\log(k) - 2\delta k + a\cos\left(2\pi \frac{k}{k_p}\right). \tag{11}$$

The least square fit equations determining the values of the parameters C, n, δ and a are linear but the one determining k_p is non-linear. In practice we determine C, n, δ and a for an assumed value of k_p and search for the minimum of the sum of the square of the errors as a function of k_p.

Note that assuming interferences from two complex singularities with the same value of δ but spatial positions differing by $2\delta_i$ and contrast factor a would yield contributions to the energy spectrum of the form

$$E(k) \sim \mathrm{e}^{-2\delta k}(1 + a\cos 2\delta_i k). \tag{12}$$

Expanding the log of this expression to the first order in a yields the additional term present in (11), with $k_p = \pi/\delta_i$.

The presence of a contrast factor may be understood, as in optics, by considering interfering singularities that are not punctual but extended objects. Indeed there is good numerical evidence (Frisch et al., 2003) that complex singularities of the two-dimensional Euler equations arere situated on regular $1D$ manifolds. Note that, in the case of the viscous 1-D Burgers equation, where the nature of the complex singularities (isolated poles) is well-understood, there is another way than the present fitting procedure to disentangle the information on δ from the oscillating energy spectrum (Kida, 1986). However in the Burgers case the contrast factor a is constantly high.

The residual oscillating part of the data, together with the fit, are displayed in Fig. 4. It is clear by inspection of the figure that the quality of the fit is correct.

It is apparent in Fig. 5 that the erratic behavior of δ and n manifest in Fig. 3 has been corrected by the extended fit (11). Perhaps the most salient effect is observed on n. The resolution dependent sharp maxima of n visible in Fig. 3 are not present in Fig. 5. The corresponding behavior of δ has also been smoothed out.

The fitted singularity separation parameter $\delta_i = \pi/k_p$ and amplitudes a are also presented in Fig. 5. δ_i appears to decay exponentially in time (with $\delta_i(t) = 0.30\mathrm{e}^{-t/0.271}$ up to a time $t = 1.25$ at resolution 2048^3). The amplitudes have resolution dependent maxima that happen at the same time than the resolution dependent maxima of the uncorrected n (see Fig. 3). It is easy to check out that these maxima happen when $k_p \sim k_{\max}$.

This point is easily understood as follows. When $k_p \ll k_{\max}$, the oscillations are averaged out in the uncorrected fit (8) and both corrected and uncorrected fits give the same values of n and δ. In the opposite regime $k_p \gg k_{\max}$ no oscillations can be detected on the available data. In the intermediate regime, when k_p approaches $k_{\max}$ from below, the curvature of the spectrum caused by the oscillation is seen by the
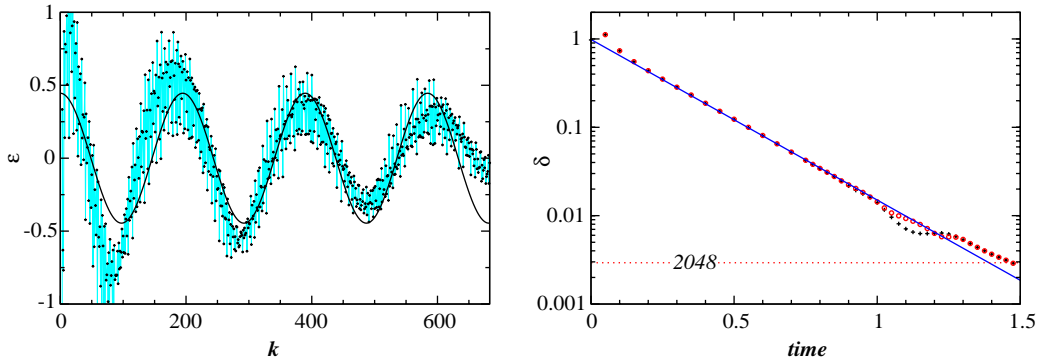
Fig. 4. Left: Fit of spectral oscillations of KP flow ($t = 0.8$, resolution 2048^3) dots: residual $\varepsilon = \log(E(k, t)) - (C - n\log(k) - 2\delta k)$; solid line: amplitude term $a\cos(2\pi\frac{k}{k_p})$ (see Eq. (11)). Right: time evolution of uncorrected decrement δ (Eq. (8): cross +), corrected decrement (Eq. (11), circle ∘) and its exponential fit from $t = 0.1$ to $t = 1.25$ (solid line).
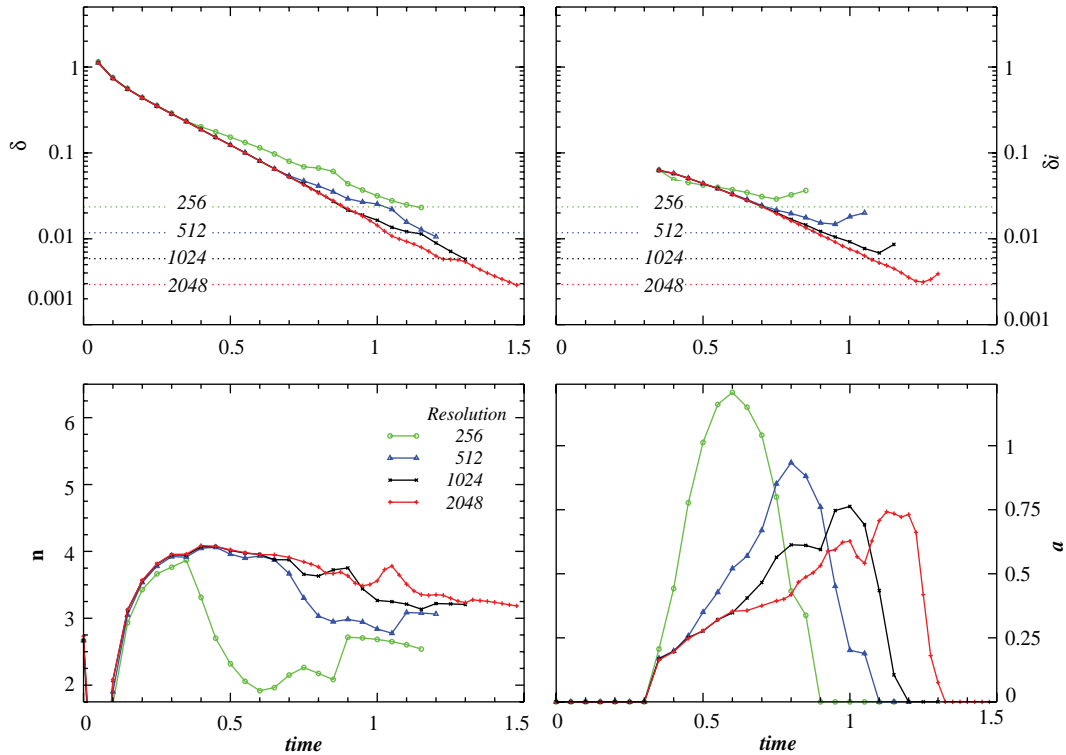

Fig. 5. Time evolution of corrected decrement δ, corrected prefactor n, oscillation amplitude a and separation parameter $\delta_i = \pi/k_p$ for KP flow at various resolutions N (see Eq. (11)). Fits are performed within the intervals $k = 5$ to $\min(k^*, N/3)$, where $k^* = \min_{E(k) < 10^{-32}}(k)$ marks the beginning of roundoff noise at short times.
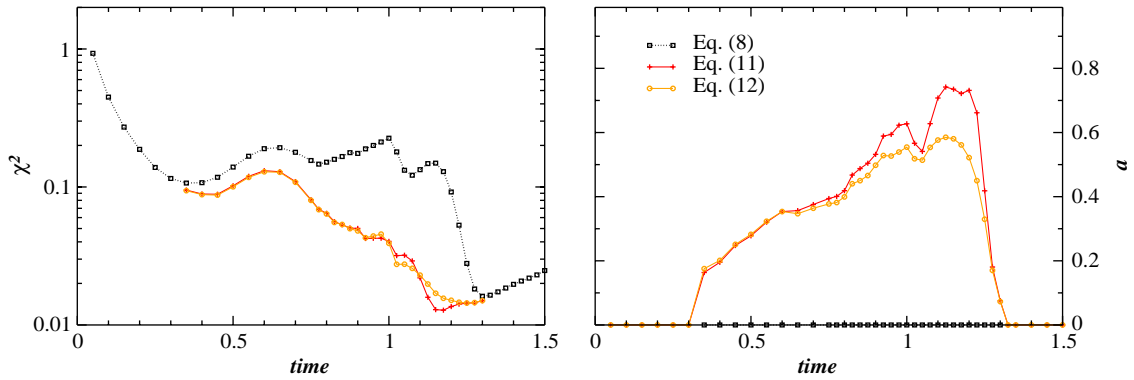
Fig. 6. Left: quadratic error χ^2, normalized by the number of fitted points, corresponding to the 3 different least-square fits at resolution 2048^3. Right: comparison of amplitudes a. Square, Eq. (8); cross, Eq. (11); circle, Eq. (12).

uncorrected fit as a change in the n term in (8). The corrected fit (11) does a better job separating out, in this regime, the oscillation from the curvature.

Using the data on δ obtained from the corrected fit (see Fig. 4), we obtain that $\delta(t)$ decays like

$$\delta(t) = \delta_0^{\mathrm{KP}} \mathrm{e}^{-t/T_{\mathrm{KP}}} \tag{13}$$

with a characteristic decay time $T_{\mathrm{KP}} = 0.24$ and $\delta_0^{\mathrm{KP}} = 1.02$, up to a time $t = 1.25$ at resolution 2048^3, where the corrected fit begins to be affected.

By inspection of Fig. 5 it is apparent that the amplitude a of the fit near its maxima almost reaches one, which is not consistent with the approximation (i.e. using $a \ll 1$ to expand the log of (12)) needed to derive (11). This suggests that a fit using the logarithm of (12) may give an even better result. In order to investigate this point, we have performed these logarithmic fits. Note that this necessitates to search for the minimum of a 2-parameter function (see the discussion below Eq. (11)).

The results are presented in Fig. 6. It is apparent, by inspection of the figure, that the quality of the fit, measured by the quadratic error χ^2, normalized by the number of fitted points, is much improved when the oscillations are taken into account. However, the level of improvement is not sensibly changed by replacing the 1-parameter non-linear fit Eq. (11) by the 2-parameter non-linear fit Eq. (12). The behavior of δ and n are not sensibly affected (data not shown) but the amplitude a is decreased when using the logarithm of (12).

4. Conclusion

In summary, complex singularities in DNS (resolutions up to 2048^3) of TG and KP flows, have been traced, using the analyticity strip method. The energy spectra fit procedure had to be generalized to take into account oscillations caused by interferences between complex singularities. Exponential-in-time decay of δ is found for both flows.

The temporal Taylor series expansions estimates for the Pelz singularity time t_{P}^* given by Pelz (2003), Pelz and Gulak (1997a, b), Boratav and Pelz (1994b) are $t_{\mathrm{P}}^* \sim 2$.

We now estimate, using data generated by the present DNS with resolution up to 2048^3, how much resolution is needed to reach t_P^*, assuming that the exponential regime (13) persists in time. The condition that $\delta k_{max} = 2$ reads $\delta k_{max} = N/3\delta_0^{KP}e^{-t_P^*/T_{KP}} = 2$ and its solution is $N = 6e^{2/T_{KP}}/\delta_0^{KP} = 24\,472$. Note that the same condition $\delta_i k_{max} = 2$ applied to the imaginary part of singularities yields $N = 32\,074$, a more stringent condition.

Thus DNS performed with resolutions in the range 16384^3–32768^3 would really probe the Pelz singularity at $t_P^* \sim 2$. Assuming a real singularity at this time, they should display a numerically-reliable faster-than-exponential decay of $\delta(t)$.

General periodic turbulent flows have been simulated with resolutions up to 4096^3 on the Earth Simulator (Kaneda et al., 2003). Efficient implementation of the TG and KP symmetries reduce memory storage and speed up computation allowing a gain in resolution up to a factor 4 in each spatial direction (Brachet et al., 1983). Thus KP simulations with resolutions 16384^3 are within reach of the Earth Simulator.

Acknowledgements

References

Boratav, O.N., Pelz, R.B., 1994a. Direct numerical simulation of transition to turbulence from a high-symmetry initial condition. Phys. Fluids 6 (8), 2757–2784.

Boratav, O.N., Pelz, R.B., 1994b. Evidence for a real-time singularity in hydrodynamics from time series analysis. Phys. Rev. Lett. 79, 4998–5001.

Brachet, M.E., Meiron, D.I., Orszag, S.A., Nickel, B.G., Morf, R.H., Frisch, U., 1983. Small-scale structure of the Taylor–Green vortex. J. Fluid Mech. 130, 411–452.

Brachet, M.E., Meneguzzi, M., Vincent, A., Politano, H., Sulem, P.L., 1992. Numerical evidence of smooth self-similar dynamics for three-dimensional ideal flows. Phys. Fluids A 4, 2845–2854.

Frisch, U., Matsumoto, T., Bec, J., 2003. Singularities of Euler flow? not out of the blue! J. Stat. Phys. 113, 761–781.

Gottlieb, D., Orszag, S.A., 1977. Numerical Analysis of Spectral Methods. SIAM, Philadelphia.

Kaneda, Y., Ishihara, T., Yokokawa, M., Itakura, K., Uno, A., 2003. Energy dissipation rate and energy spectrum in high resolution direct numerical simulations of turbulence in a periodic box. Phys. Fluids 15, 121–124.

Kerr, R.M., 1993. Evidence for a singularity of the three-dimensional incompressible Euler equations. Phys. Fluids A 5, 1725–1746.

Kida, S., 1985. Three-dimensional periodic flows with high symmetry. J. Phys. Soc. Japan 54, 2132–2136.

Kida, S., 1986. Study of complex singularities by filtered spectral method. J. Phys. Soc. Japan 55, 1542–1555.

Pelz, R.B., 2001. Symmetry and the hydrodynamic blowup problem. J. Fluid Mech. 444, 343–382.

Pelz, R.B., 2003. Extended series analysis of full octahedral flow: numerical evidence for hydrodynamic blowup. Fluid Dynam. Res. 33, 207–221.

Pelz, R.B., Gulak, Y., 1997a. Evidence for a real-time singularity in hydrodynamics from time series analysis. Phys. Rev. Lett. 25, 4998–5001.

Pelz, R.B., Gulak, Y., 1997b. Locally self-similar finite-time collapse in a high-symmetry vortex-filament model. Phys. Rev. E 55, 1617–1626.

Sulem, C., Sulem, P.L., Frisch, H., 1983. Tracing complex singularities with spectral methods. J. Comput. Phys. 50 (1), 138–161.

Taylor, G.I., Green, A.E., 1937. Mechanism of the production of small eddies from large ones. Proc. Roy. Soc. London A 158, 499–521.